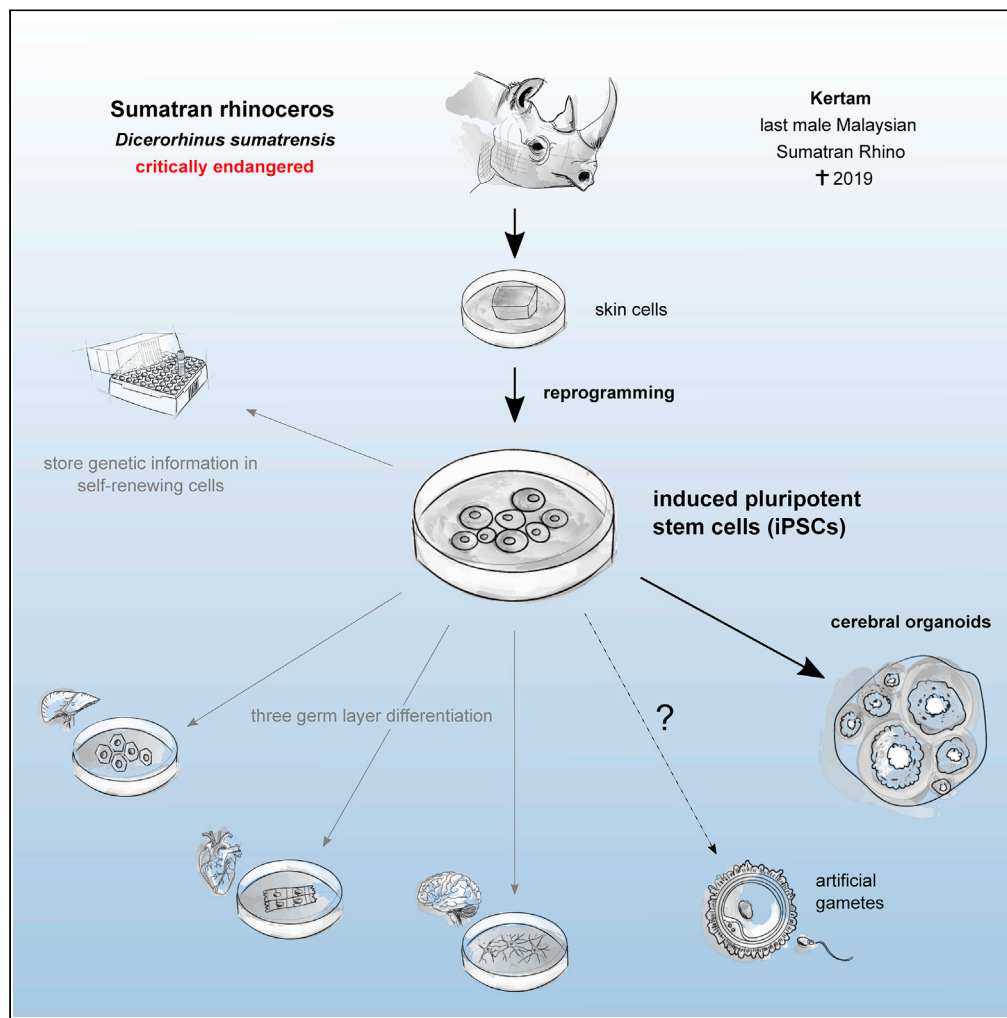


Article

Induced pluripotent stem cells and cerebral organoids from the critically endangered Sumatran rhinoceros



Vera Zywitzka, Silke Frahm, Norman Krüger, ..., Micha Drukker, Thomas B. Hildebrandt, Sebastian Diecke

sebastian.diecke@mdc-berlin.de

Highlights

Characterization of Sumatran Rhino (SR) fibroblasts

Generation of SR induced pluripotent stem cells (SR-iPSCs)

SR-iPSCs generate cells of the three germ layers

SR-iPSCs give rise to cerebral organoids

Zywitzka et al., iScience 25, 105414
November 18, 2022 © 2022 The Authors.
<https://doi.org/10.1016/j.isci.2022.105414>



Article

Induced pluripotent stem cells and cerebral organoids from the critically endangered Sumatran rhinoceros

Vera Zywitzka,¹ Silke Frahm,¹ Norman Krüger,¹ Anja Weise,² Frank Göritz,³ Robert Hermes,³ Susanne Holtze,³ Silvia Colleoni,⁴ Cesare Galli,^{4,5} Micha Drukker,^{6,8} Thomas B. Hildebrandt,^{3,7} and Sebastian Diecke^{1,9,*}

SUMMARY

Less than 80 Sumatran rhinos (SR, *Dicerorhinus sumatrensis*) are left on earth. Habitat loss and limited breeding possibilities are the greatest threats to the species and lead to a continuous population decline. To stop the erosion of genetic diversity, reintroduction of genetic material is indispensable. However, as the propagation rate of captive breeding is far too low, innovative technologies have to be developed. Induced pluripotent stem cells (iPSCs) are a powerful tool to fight extinction. They give rise to each cell within the body including gametes and provide a unique modality to preserve genetic material across time. Additionally, they enable studying species-specific developmental processes.

Here, we generate iPSCs from the last male Malaysian SR Kertam, who died in 2019, and characterize them comprehensively. Differentiation in cells of the three germ layers and cerebral organoids demonstrate their high quality and great potential for supporting the rescue of this critically endangered species.

INTRODUCTION

The Sumatran rhino (SR, *Dicerorhinus sumatrensis*), also known as hairy or Asian two-horned rhino, is the smallest and most ancient of five extant rhinoceros species.¹ Once, it inhabited a continuous, vast area in East and Southeast Asia, but now only small, fragmented populations remain scattered across Sumatra and Indonesian Borneo. The current stock is estimated at 40–78 individuals distributed over up to ten sub-populations,² which increases the risks of inbreeding and asymmetric reproductive ageing-related female infertility, i.e. development of reproductive tract pathologies as a result of repeated ovarian cycling activity due to the absence of naturally occurring long acyclic gestation and lactation phases.³ Reintroduction of genetic material is crucial to support a healthy and self-sustaining SR population. Contrary, the classical captive breeding approach in the USA, Malaysia, and Indonesia only led to five offspring from a total of 47 individuals since the first SRs were received in captivity for breeding purposes in 1985 (Sumatran Rhino Crisis Summit, Singapore Zoo, 1–4 April 2013) highlighting the need for the future application of advanced assisted reproduction technologies.⁴ Toward this aim, we will employ adult, somatic cells to generate induced pluripotent stem cells (iPSCs),⁵ which - in contrast to primary cells - are capable of unlimited expansion and therefore a valuable tool to store the genetic information of endangered species across time. Additionally, iPSCs can make each cell type of a body including oocytes and spermatozoa,⁶ which in turn could be used for *in vitro* fertilization thereby contributing to breeding of infertile or already deceased individuals.^{4,7} Generation of fertile and viable offspring from iPSCs has successfully been demonstrated for mice,^{8,9} and the process is increasingly applied to a variety of other mammalian species. *In vitro* differentiation of primordial germ cell-like cells (PGCLCs), the precursors of oocytes and spermatozoa, has been reported for humans, cynomolgus monkeys, and rabbits,^{10–13} raising the hope that the modality will also be applicable to endangered species such as the SR.

Beyond application in innovative conservation strategies, iPSCs from endangered species enable studying species-specific developmental processes. As embryonic material from exotic, large mammals is very limited to almost inaccessible, iPSCs are an unprecedented tool to gain insights into embryo- and organogenesis.

¹Max-Delbrück-Center for Molecular Medicine in the Helmholtz Association (MDC), Technology Platform Pluripotent Stem Cells, 13125 Berlin, Germany

²Institute of Human Genetics, Jena University Hospital, Friedrich Schiller University, 07747 Jena, Germany

³Leibniz Institute for Zoo and Wildlife Research, 10315 Berlin, Germany

⁴Avantea, 26100 Cremona, Italy

⁵Fondazione Avantea, 26100 Cremona, Italy

⁶Helmholtz Zentrum München, Institute of Stem Cell Research, 85764 Neuherberg, Germany

⁷Freie Universität Berlin, Faculty of Veterinary Medicine, 14163 Berlin, Germany

⁸Present address: Leiden University, Division of Drug Discovery and Safety, Leiden Academic Centre for Drug Research (LACDR), 2300 RA Leiden, the Netherlands

⁹Lead contact

*Correspondence: sebastian.diecke@mhc-berlin.de

<https://doi.org/10.1016/j.isci.2022.105414>



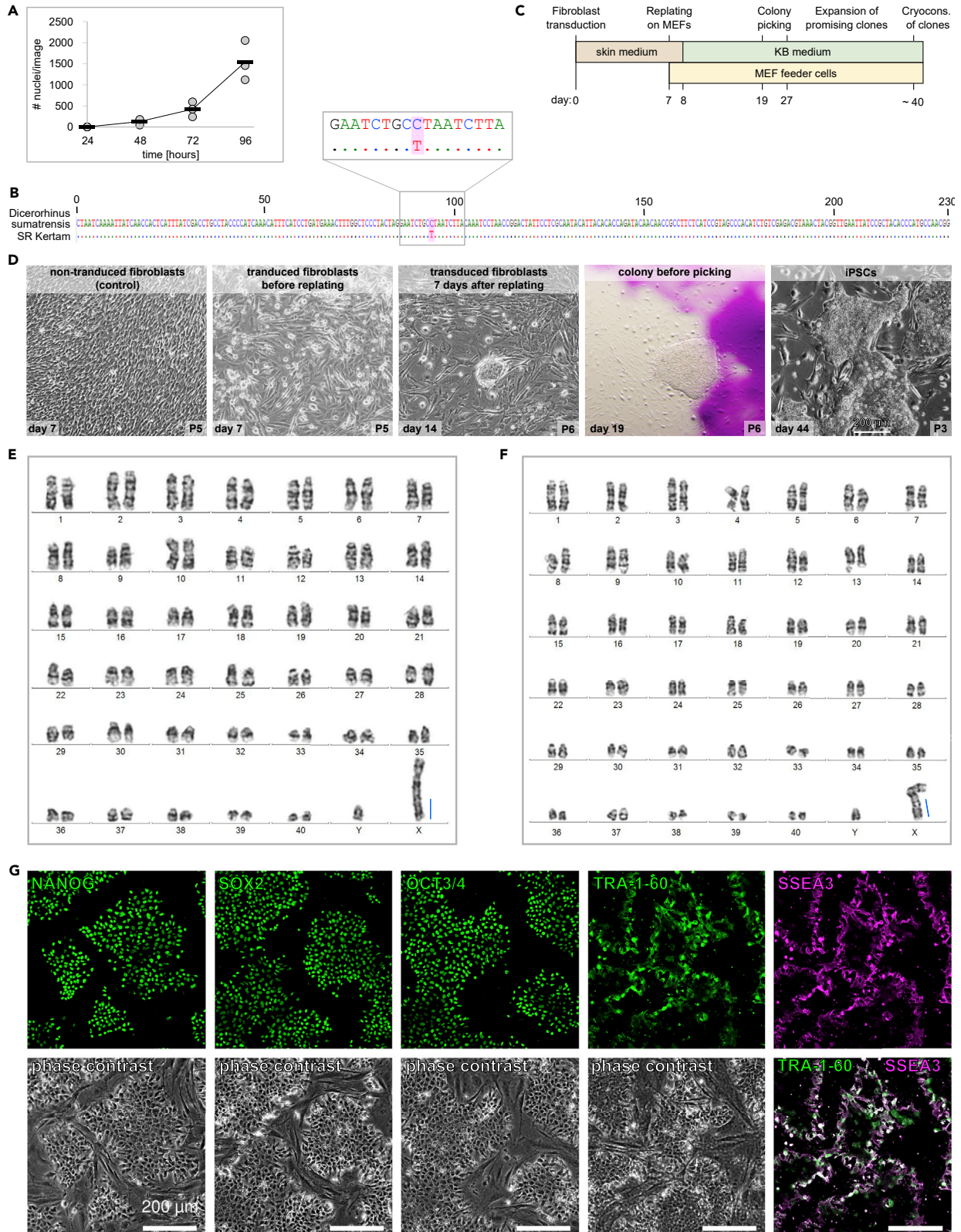


Figure 1. Generation of SR-iPSCs

(A) Proliferation analysis. Stained nuclei of cells fixed at 24h, 48h, 72h, and 96h after plating were counted in three images per timepoint (one per 24 well). The slope between 48h and 96h was used to determine the population doubling time. Each circle represents the value of each replicate per time point. Line depicts the mean.

(B) Species analysis based on amplification and Sanger-sequencing of a 230 bp cytochrome-b region, according to.¹⁴ Top line: reference sequence. Close up of region with 1 bp substitution (highlighted in pink).

(C) Timeline of reprogramming.

(D) Cell images during reprogramming of SR Kertam fibroblasts (10x magnification). Scale bar image far right: 200 μ m.

(E and F) Exemplarily G-banded karyotypes of SR Kertam fibroblasts (E) and iPSCs (F). $2n = 82$, including Y and X chromosomes. Blue bar indicates the addition of heterochromatin near the q terminal ends of the X chromosome.

(G) Immunostaining of pluripotency markers. Upper lane: marker only. Lower lane: phase contrast. Bottom far right: merge TRA-1-60 and SSEA3. Scale bars: 200 μ m.

See also [Figures S1](#) and [S2](#).

Here, we generate iPSCs from the SR Kertam, who was the last male Malaysian SR before his death at Tabin Wildlife Reserve in 2019. We characterize both source fibroblasts and iPSCs thoroughly and demonstrate three-germ layer differentiation potential of the latter. The generation of cerebral organoids from SR-iPSCs highlights their ability to generate complex 3D structures, and concomitantly represents a promising application for studying the evolutionary progression of brain development across species. Taken together, this work represents the first step towards fighting the extinction of the SR using stem cell-associated techniques (SCAT).

RESULTS**Generation and characterization of Sumatran rhino-induced pluripotent stem cells**

In 2019, the Sumatran rhino (SR) was declared extinct in Malaysia. The last three individuals, Puntung, Imam (both female), and Kertam (male) were housed at Tabin Wildlife Reserve in Lahad Datu, Malaysia, and great efforts have been made to breed them in captivity. Even after Kertam's death, an *in vitro* fertilization attempt using his cryopreserved sperm has been made. However, Imam's isolated oocytes failed to divide after fertilization, probably due to the poor quality of Kertam's cryopreserved spermatozoa. To preserve the genetic material and to retain the possibility to obtain viable sperm cells from Kertam in future, we generated induced pluripotent stem cells (iPSCs). Therefore, we took a skin biopsy under general anesthesia and isolated fibroblasts. Cryopreserved SR-fibroblasts grew well after thawing and had a population doubling time of 19 h during the logarithmic phase of growth (48–96 h, [Figure 1A](#)). To confirm their identity, we sequenced a 230 bp cytochrome-b region, which can be used to discriminate the five extant rhinoceros species.¹⁴ Except for one substitution (C \rightarrow T), the amplified DNA mapped unambiguously to the SR-reference sequence ([Figure 1B](#)). To generate iPSCs, we used an adapted protocol that has been optimized recently for reprogramming northern white rhino (NWR, *Ceratotherium simum cottoni*) fibroblasts (Hayashi et al., *submitted*¹⁵; [Figure 1C](#)). Therefore, SR-fibroblasts were plated at low density in skin media and two days later transduced with Sendai-Viruses encoding the human reprogramming factors *POU5F1*, *SOX2*, *KLF4* and *c-MYC*. Similar to NWR-fibroblasts, SR-fibroblasts were less susceptible to viral transduction than human fibroblasts. A two times higher viral concentration as recommended for human cells worked well ([Figure 1D](#), day 7). Within 7 days after transduction, the characteristic mesenchymal to epithelial transition (MET) became apparent, which was accompanied by morphological transformation from spindle- to planar-shaped with high nucleus to cytoplasm ratio. On day 7, cells were replated on mitotically inactivated mouse embryonic fibroblasts (MEFs) and feeder-free on Geltrex-coated dishes. The day after, cultures on MEFs were changed to KB medium, whereas feeder-free cultures were changed to mTeSR1. Individual colonies of tightly packed cells with prominent nucleoli were observed from 14 days after transduction on and were isolated from both conditions on days 19 and 21. Similar to reprogramming of NWR-iPSCs, SR-iPSC lines could only be established with the KB on MEFs condition. However, once stabilized, NWR-iPSC lines could be adapted to feeder-free mTeSR1¹⁵ or rather mTeSR1:KB medium (Hayashi et al., *submitted*), whereas SR-iPSCs spontaneously differentiated or died in all tested feeder-free conditions. To assess the genetic integrity of SR-fibroblasts and SR-iPSCs, we performed karyotyping by GTG banding and observed a diploid chromosome number of $2n = 82$ comprising 80 acrocentric autosomes and two gonosomes (X and Y) in both cell types. As described previously,¹⁶ the X chromosome contained a conspicuous long q arm (blue bar [Figures 1E](#) and [1F](#)), which demonstrably consists of heterochromatin (CGB banding, [Figure S1](#)). The absence of expression of exogenous reprogramming factors was confirmed by RT-PCR ([Figure S2](#)). SR-iPSCs expressed the canonical pluripotency markers NANOG, SOX2, OCT3/4 as well as the pluripotency surface markers TRA-1-60 and SSEA3 ([Figure 1G](#)).

Three germ-layer differentiation potential of Sumatran rhino-induced pluripotent stem cells

Next, we demonstrated the pluripotent potential of SR-iPSCs by generating cells of the three germ layers using protocols optimized for directed differentiation of human PSCs. Definitive endoderm progenitors were efficiently generated after 5 days of culture in the differentiation medium, and their identity was confirmed by immunostaining of GATA4, GATA6, and SOX17 (Figure 2A). To represent the mesoderm, SR-iPSCs were differentiated into beating cardiomyocytes. Clusters of beating cells were observed 9 days after the start of differentiation.

The cells expressed the cardiac-specific proteins ACTN2 and TNNT2 (Figure 2B). Towards ectoderm, we differentiated SR-iPSCs into neural progenitor cells and at day 12 of differentiation observed the formation of neural rosettes expressing SOX2, NES, and SOX1 (Figure 2C). To confirm the specificity of signal, we performed immunostaining excluding primary antibodies (negative control) and imaged background signals derived from secondary antibodies only (Figure 2D).

Sumatran rhino cerebral organoids

Little is known about the rhino brain and its development during embryogenesis. In 1878, the morphology of the SR brain has been described¹⁷ and it seems that not much more is presently known about the brain of the species. The main reason for this lack of knowledge is probably the absence of biological material that can be studied. Much of our understanding of human-specific neural development arose in the last years, since the generation of three-dimensional cerebral organoids from great ape iPSCs opened entirely new possibilities to study early brain expansion and neurogenesis.^{18,19} Besides great apes, to the best of our knowledge only mouse brain organoids have been generated from embryonic stem cells so far.^{20,21} These recapitulated the spatial and temporal aspects of *in vivo* rodent corticogenesis, validating organoids as tools to study brain development. Thus, the generation of SR cerebral organoids opens unprecedented possibilities to study rhino neurogenesis.

Having established the neural induction of SR-iPSCs (Figure 2C) using small molecules designed for human NPC differentiation, we thought to employ a standard protocol for cerebral organoid generation.¹⁸ Standard single-cell seeding did not result in the formation of embryoid bodies (EBs) containing neuroectodermal structures from SR-iPSCs (not shown) in contrast to human iPSCs (Figure S3A). Therefore, we modified the protocol and exchanged the enzymatic single-cell seeding at day 0 for a cluster split using a non-enzymatic dissociation procedure. The resulting small aggregates of variable size (100–300 μm in diameter) resembled EBs and developed optically translucent tissue at the margin between days 5 and 7, indicating the induction of neuroectoderm (Figure 3A). Further addition of 2% Matrigel to the medium gave rise to radially organized neuroepithelium (a hallmark of human brain organoids) in both, rhino and human organoids (days 10–13; Figures 3 and S3). Immunostaining of SR brain organoids at 1 month of age confirmed the formation of well-defined progenitor zones expressing SOX2, some of which were positive for the dorsal cortical marker PAX6 (Figure 3B). Accordingly, SR organoid tissue displayed neurons distal to the progenitor zones which stained positive for the pan-neuronal marker MAP2, the cortical neuronal markers BRN2 and CTIP2, and the hippocampal marker PROX1 (Figure 3B), comparably to human organoids generated with the same kit (Figure S3B). After additional 2 months in culture, we observed GFAP-positive astrocytes lining the outer surface of the organoids, as described before in self-organized human cerebral organoids.²² Moreover, 3-month old in comparison to 1-month-old organoids exhibited more CTIP2-positive neurons, which were lined by SATB2-positive neurons, indicating further maturation.

DISCUSSION

The sixth mass extinction, which is caused by human activities, is progressing with unprecedented speed.^{23,24} Notably, the five extant rhinoceros species are particularly affected due to poaching, habitat destruction, and fragmentation. Loss of keystone species, especially megavertebrates, can initiate so-called “vortex effects,”²⁵ i.e. accelerated loss of species or entire species societies whose life histories are directly or indirectly connected to the keystone species. The Sumatran Rhino (SR) is known to play a key role in shaping forests and spreading seeds of at least 79 different plant species.²⁶ Many of those evolved alongside megafauna and are designed to be eaten and dispersed by large animals such as elephants and rhinos. Given the differences in ranging and foraging behavior of SRs and elephants, and the fact that 35% of the identified megafaunal fruits are only distributed by SRs,²⁶ the composition and ecological balance of the Asian rainforest seem highly dependent on the SR and loss of the species could have catastrophic consequences.

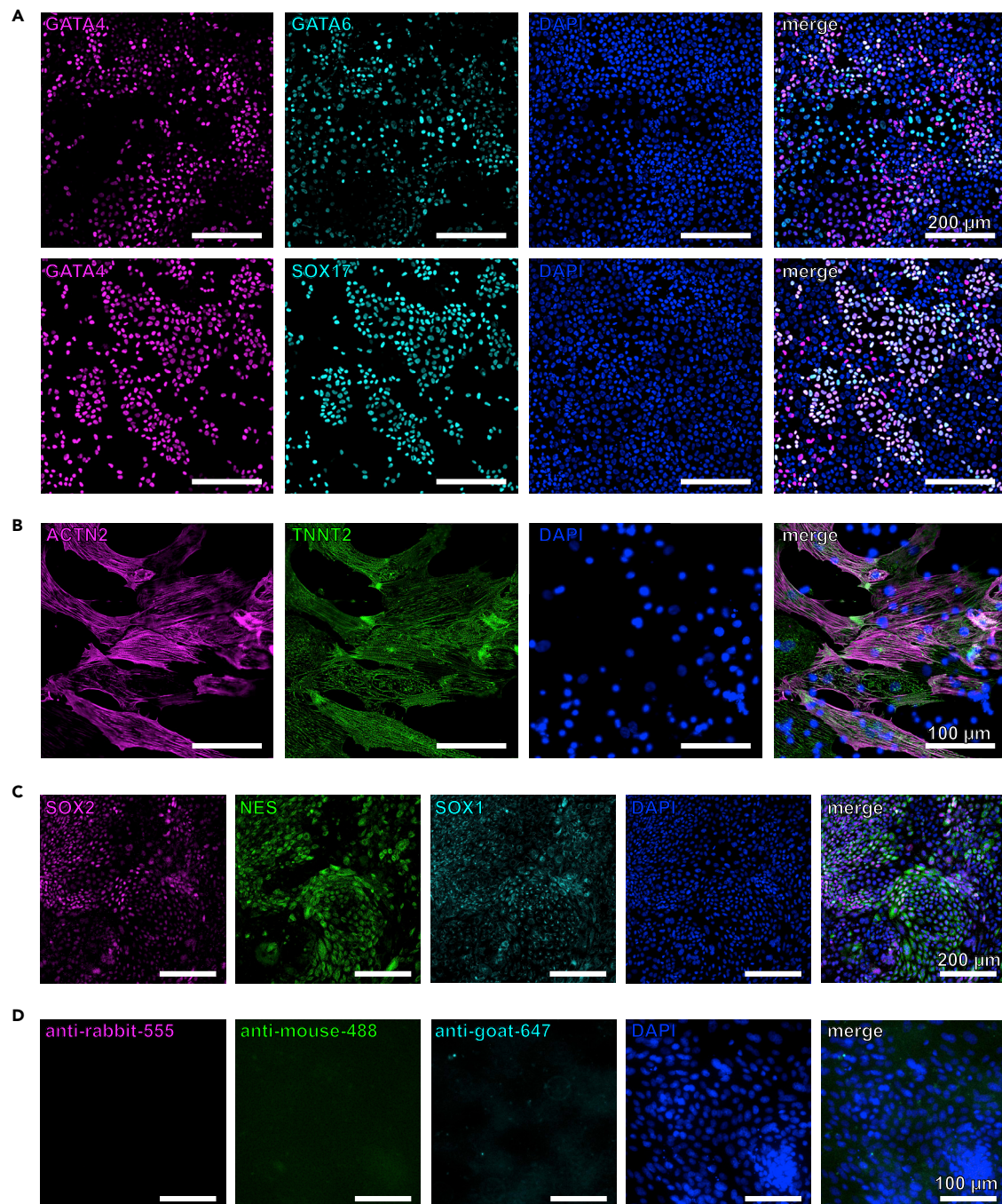


Figure 2. SR-iPSCs generate cells of the three germ layers

(A–C) Representative immunostainings for markers of the three germ layers upon differentiation of SR-iPSCs towards endoderm (A), cardiomyocytes (mesoderm, B), and neural precursors (ectoderm, C).

(D) Negative control: to confirm the specificity of signal, immunostaining of neural precursors was performed excluding primary antibodies. Cells were stained with secondary antibody only. For imaging, the same exposure times as applied in panel C were used. Scale bars: 200 μm (A, C) and 100 μm (B, D).

To fight the extinction of the SR, great efforts worldwide - particularly by the Indonesian government and international partners - are made to increase its population. Recently, on March 24, 2022, the rare event of a SR calf born in captivity has been reported by Indonesia's Ministry of Environment. However, the numbers

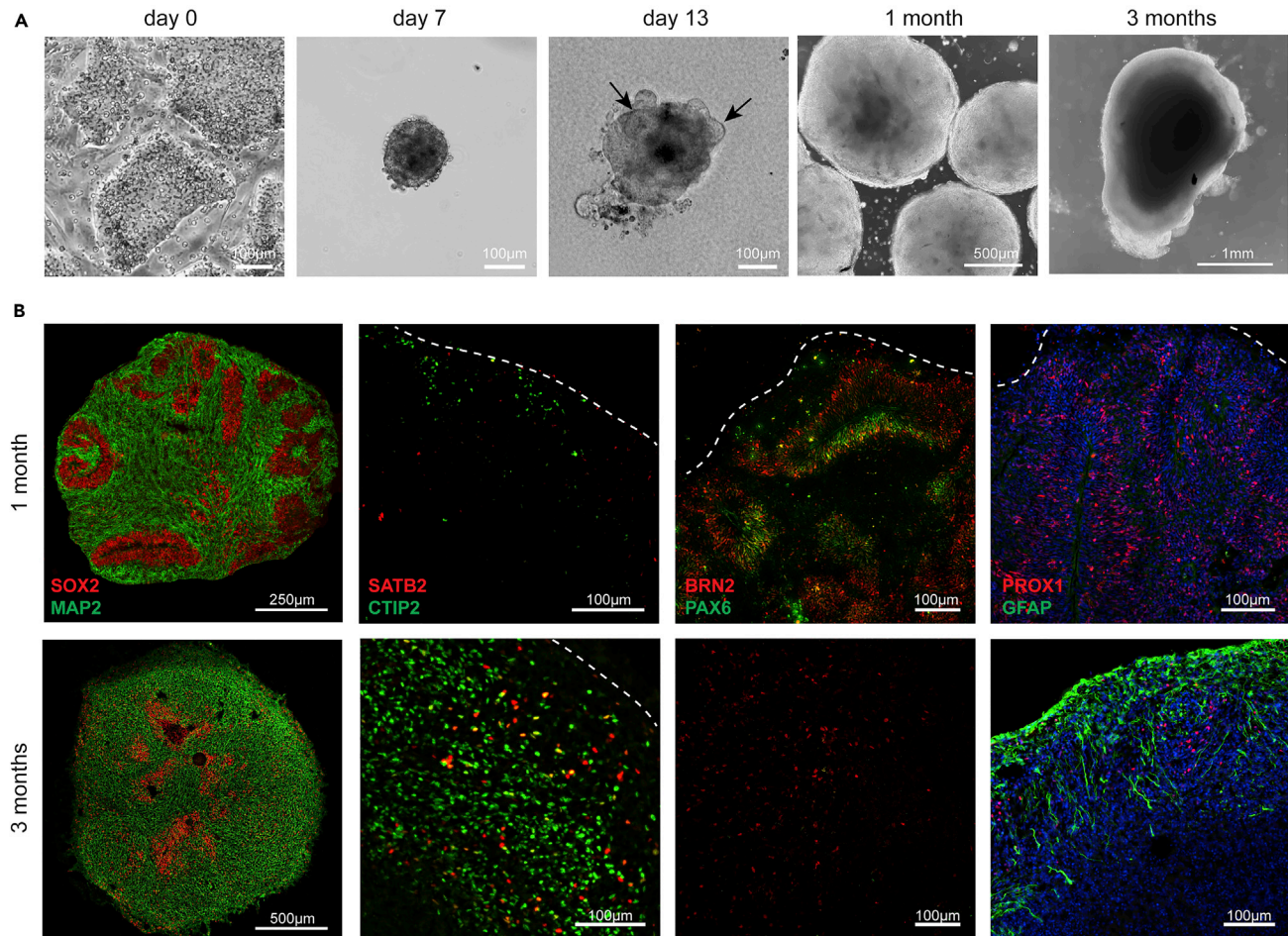


Figure 3. SR cerebral organoids

(A) Exemplary phase contrast images during organoid generation at corresponding days of differentiation. Day 0: feeder-dependent SR-iPSC colonies before dissociation; day 7: embryoid body showing a smooth and brightened surface; day 13: after the addition of Matrigel to the medium, organoids showed neuroepithelial bud outgrowth resembling neural tube-like structures (arrows), which are still visible after 1 month in culture. 3 months: mature organoid. Scale bars are defined within each image.

(B) Immunostaining of 1 (top panels) and 3 (lower panels) months old SR brain organoids. Radially organized neural progenitors stain positive for SOX2 and PAX6, while neurons express MAP2, CTIP2, SATB2, BRN2, and PROX1. Astrocytes appear in older organoids and express GFAP. Scale bars are defined within each image.

See also [Figure S3](#).

of both fertile individuals and successful breeding in captivity remain low, and highlight the need to explore innovative alternatives.

Stem cell-associated techniques (SCAT) in combination with advanced assisted reproduction technologies (aART) open up new perspectives to rescue endangered species.⁴ By generating induced pluripotent stem cells (iPSCs) from the SR Kertam, who was the last male Malaysian SR and belonged to the Bornean subspecies, we conserved his genetic information, and created an opportunity to produce viable spermatozoa for breeding purposes in future. As the quality of semen collected from SRs is poor directly after retrieval and even worse after cryopreservation and thawing,²⁷ *in vitro* generated spermatozoa offer a great alternative for assisted breeding of SRs in general.

In addition, we demonstrate the applicability of iPSCs obtained from endangered species to study species-specific developmental processes by differentiating cerebral organoids from SR-iPSCs. Our experiments show that SR cerebral organoids develop in a self-organized manner, and express all neural markers tested

(selection of eight markers commonly reported in human iPSC-derived brain organoids). Thus, cortical organoid development from SR and human iPSCs is seemingly comparable regarding differentiation into neural stem cells and consecutively into neurons and astrocytes. However, a side-by-side comparison of age-matched SR and human brain organoids is not applicable using the data obtained, since the generation of SR-iPSC-derived EBs during the first days of differentiation did not succeed in the culture conditions used for human iPSCs and needed to be adapted. Only a non-enzymatic dissociation of SR-iPSC into clusters and culturing in KB medium yielded aggregates that formed EBs (instead of culturing a single cell suspension in EB medium). As a consequence, the size of the EBs formed after 5 days in culture was not uniform and overall smaller as compared to human iPSC-derived EBs, which in turn lead to differences in the number of neuroepithelial buds and neural tube-like structures (SOX2-positive rosettes) observed between species. However, due to the technical modification, this variation should not be considered to be genetic in origin. Nevertheless, SR and human organoids were cultured under the same conditions after neural induction and therefore neurogenesis could be studied and compared qualitatively between species. For example, SR and human organoids both expressed the postmitotic cortical markers CTIP2 and SATB2 at later stages, indicative of neuronal maturation. Notably, the timing of SATB2 transcriptional activity defines axonal projection routes exclusive in eutherian mammals, which is relevant for the evolution and development of cortical circuits.²⁸ Previous work with brain organoids from different species has shown that differential temporal expression dynamics of other conserved transcription factors can also have a profound impact on brain expansion.¹⁹ Thus, using comparative RNA-sequencing, SR brain organoids could contribute to study the evolutionary progression of brain development in mammals beyond mouse/human interspecies differences and may help to unravel the ancient history of the rhinoceros family.

Limitations of the study

As mentioned in the discussion, a quantitative side-by-side comparison of age-matched SR and human brain organoids is not possible with the data presented in this study, because different experimental set-ups had to be used for organoid generation. The here presented method to generate SR organoids allows for the qualitative comparison of human and SR brain organoids, however, for a quantitative comparison, the set-up would need to be adjusted.

STAR★METHODS

Detailed methods are provided in the online version of this paper and include the following:

- KEY RESOURCES TABLE
- RESOURCE AVAILABILITY
 - Lead contact
 - Materials availability
 - Data and code availability
- EXPERIMENTAL MODEL AND SUBJECT DETAILS
 - Sumatran rhinoceros kertam
 - Human cell lines
- METHOD DETAILS
 - Derivation of SR primary fibroblast
 - Species analysis
 - Proliferation analysis
 - Generation of SR-iPSCs
 - Clearance of sendai-virus encoded RNA
 - SR-iPSC maintenance culture
 - Karyotyping of SR-iPSCs
 - Three germ layer differentiation potential
 - Cerebral organoids
 - Cryosectioning of cerebral organoids
 - Immunofluorescence
- QUANTIFICATION AND STATISTICAL ANALYSIS

SUPPLEMENTAL INFORMATION

Supplemental information can be found online at <https://doi.org/10.1016/j.isci.2022.105414>.

ACKNOWLEDGMENTS

We thank our Malaysian colleagues Dr John Payne and Dr Zainal Zahari Zainuddin for the fruitful collaboration, and our colleagues from Diecke lab for technical assistance, especially Maren Wendt for her great efforts in the immunohistochemistry of organoids. This work was supported in part by grants from the Malaysian non-governmental organization Sime Darby Foundation and from the German government (BMBF 01LC1902B BioRescue), as well as by Richard McLellan and his non-governmental organization "Rewind Rhino Extinction."

AUTHOR CONTRIBUTIONS

Conceptualization, T.B.H., S.D., C.G., and M.D.; Validation, V.Z., S.F., and A.W., Methodology, V.Z. and S.F.; Investigation, V.Z., S.F., N.K., A.W., and S.C.; Resources, F.G., R.H., S.H., and T.B.H.; Writing – Original Draft, V.Z. and S.F., Writing – Review & Editing, V.Z., S.F., T.B.H., S.H., and S.D., Funding Acquisition, T.H.B. and S.D.

DECLARATION OF INTERESTS

The authors declare no competing interests.

INCLUSION AND DIVERSITY

We support inclusive, diverse, and equitable conduct of research.

Received: June 9, 2022

Revised: September 2, 2022

Accepted: October 18, 2022

Published: November 18, 2022

REFERENCES

- Liu, S., Westbury, M.V., Dussex, N., Mitchell, K.J., Sinding, M.-H.S., Heintzman, P.D., Duchêne, D.A., Kapp, J.D., von Seth, J., Heiniger, H., et al. (2021). Ancient and modern genomes unravel the evolutionary history of the rhinoceros family. *Cell* 184, 4874–4885.e16.
- Emslie, R., Milliken, T., Talukdar, B., Burgess, G., Adcock, K., Balfour, D., and Knight, M. (2019). CoP18 doc. 83.1 annex 2 african and asian rhinoceroses-status, conservation and trade A report from the IUCN species survival commission (IUCN SSC) african and asian rhino specialist groups and TRAFFIC to the CITES secretariat pursuant to resolution conf 9.
- Hermes, R., Hildebrandt, T.B., and Göritz, F. (2004). Reproductive problems directly attributable to long-term captivity— asymmetric reproductive aging. *Anim. Reprod. Sci.* 82–83, 49–60.
- Hildebrandt, T.B., Hermes, R., Goeritz, F., Appeltant, R., Colleoni, S., de Mori, B., Diecke, S., Drukker, M., Galli, C., Hayashi, K., et al. (2021). The ART of bringing extinction to a freeze - history and future of species conservation, exemplified by rhinos. *Theriogenology* 169, 76–88.
- Takahashi, K., Tanabe, K., Ohnuki, M., Narita, M., Ichisaka, T., Tomoda, K., and Yamanaka, S. (2007). Induction of pluripotent stem cells from adult human fibroblasts by defined factors. *Cell* 131, 861–872.
- Hayashi, K., Galli, C., Diecke, S., and Hildebrandt, T.B. (2021). Artificially produced gametes in mice, humans and other species. *Reprod. Fertil. Dev.* 33, 91.
- Saragusty, J., Diecke, S., Drukker, M., Durrant, B., Friedrich Ben-Nun, I., Galli, C., Göritz, F., Hayashi, K., Hermes, R., Holtze, S., et al. (2016). Rewinding the process of mammalian extinction. *Zoo Biol.* 35, 280–292.
- Hikabe, O., Hamazaki, N., Nagamatsu, G., Obata, Y., Hirao, Y., Hamada, N., Shimamoto, S., Imamura, T., Nakashima, K., Saitou, M., and Hayashi, K. (2016). Reconstitution in vitro of the entire cycle of the mouse female germ line. *Nature* 539, 299–303.
- Ishikura, Y., Ohta, H., Sato, T., Murase, Y., Yabuta, Y., Kojima, Y., Yamashiro, C., Nakamura, T., Yamamoto, T., Ogawa, T., and Saitou, M. (2021). In vitro reconstitution of the whole male germ-cell development from mouse pluripotent stem cells. *Cell Stem Cell* 28, 2167–2179.e9.
- Irie, N., and Surani, M.A. (2017). Efficient induction and isolation of human primordial germ cell-like cells from competent human pluripotent stem cells. *Methods Mol. Biol.* 1463, 217–226.
- Kobayashi, T., Castillo-Venzor, A., Penfold, C.A., Morgan, M., Mizuno, N., Tang, W.W.C., Osada, Y., Hirao, M., Yoshida, F., Sato, H., et al. (2021). Tracing the emergence of primordial germ cells from bilaminar disc rabbit embryos and pluripotent stem cells. *Cell Rep.* 37, 109812.
- Sakai, Y., Nakamura, T., Okamoto, I., Gyobu-Motani, S., Ohta, H., Yabuta, Y., Tsukiyama, T., Iwatani, C., Tsuchiya, H., Ema, M., et al. (2020). Induction of the germ cell fate from pluripotent stem cells in cynomolgus monkeys. *Biol. Reprod.* 102, 620–638.
- Sasaki, K., Yokobayashi, S., Nakamura, T., Okamoto, I., Yabuta, Y., Kurimoto, K., Ohta, H., Moritoki, Y., Iwatani, C., Tsuchiya, H., et al. (2015). Robust in vitro induction of human germ cell fate from pluripotent stem cells. *Cell Stem Cell* 17, 178–194.
- Ewart, K.M., Frankham, G.J., McEwing, R., Webster, L.M.I., Ciavaglia, S.A., Linacre, A.M.T., The, D.T., Ovouthan, K., and Johnson, R.N. (2018). An internationally standardized species identification test for use on suspected seized rhinoceros horn in the illegal wildlife trade. *Forensic Sci. Int. Genet.* 32, 33–39.
- Korody, M.L., Ford, S.M., Nguyen, T.D., Pivaroff, C.G., Valiente-Alandi, I., Peterson, S.E., Ryder, O.A., and Loring, J.F. (2021). Rewinding extinction in the northern white rhinoceros: genetically diverse induced pluripotent stem cell bank for genetic rescue. *Stem Cells Dev.* 30, 177–189.
- Houck, M.L., Ryder, O.A., Kumamoto, A.T., and Benirschke, K. (1995). Cytogenetics of the rhinocerotidae. *Verhandlungsbericht des Internationalen Symposiums über die Erkrankungen der Zootiere* 37, 25–32.
- Garrod, A.H. (1878). X. On the brain of the sumatran rhinoceros (*ceratorhinus sumatrensis*). *Trans. Zool. Soc. Lond.* 10, 411–414.

18. Lancaster, M.A., and Knoblich, J.A. (2014). Generation of cerebral organoids from human pluripotent stem cells. *Nat. Protoc.* *9*, 2329–2340.
19. Benito-Kwiecinski, S., Giandomenico, S.L., Sutcliffe, M., Riis, E.S., Freire-Pritchett, P., Kelava, I., Wunderlich, S., Martin, U., Wray, G.A., McDole, K., and Lancaster, M.A. (2021). An early cell shape transition drives evolutionary expansion of the human forebrain. *Cell* *184*, 2084–2102.e19.
20. Eiraku, M., Watanabe, K., Matsuo-Takasaki, M., Kawada, M., Yonemura, S., Matsumura, M., Wataya, T., Nishiyama, A., Muguruma, K., and Sasai, Y. (2008). Self-organized formation of polarized cortical tissues from ESCs and its active manipulation by extrinsic signals. *Cell Stem Cell* *3*, 519–532.
21. Nasu, M., Takata, N., Danjo, T., Sakaguchi, H., Kadoshima, T., Futaki, S., Sekiguchi, K., Eiraku, M., and Sasai, Y. (2012). Robust formation and maintenance of continuous stratified cortical neuroepithelium by laminin-containing matrix in mouse ES cell culture. *PLoS One* *7*, e53024.
22. Renner, M., Lancaster, M.A., Bian, S., Choi, H., Ku, T., Peer, A., Chung, K., and Knoblich, J.A. (2017). Self-organized developmental patterning and differentiation in cerebral organoids. *EMBO J.* *36*, 1316–1329.
23. Ceballos, G., Ehrlich, P.R., and Raven, P.H. (2020). Vertebrates on the brink as indicators of biological annihilation and the sixth mass extinction. *Proc. Natl. Acad. Sci. USA* *117*, 13596–13602.
24. Kolbert, E. (2015). *The Sixth Extinction: An Unnatural History* (Picador).
25. Lacy, R.C. (1993). VORTEX: a computer simulation model for population viability analysis. *Wildl. Res.* *20*, 45.
26. McConkey, K.R., Aldy, F., Ong, L., Sutisna, D.J., and Campos-Arceiz, A. (2022). Lost mutualisms: seed dispersal by Sumatran rhinos, the world's most threatened megafauna. *Biotropica* *54*, 346–357.
27. O'Brien, J.K., and Roth, T.L. (2000). Post-coital sperm recovery and cryopreservation in the Sumatran rhinoceros (*Dicerorhinus sumatrensis*) and application to gamete rescue in the African black rhinoceros (*Diceros bicornis*). *J. Reprod. Fertil.* *118*, 263–271.
28. Paolino, A., Fenlon, L.R., Kozulin, P., Haines, E., Lim, J.W.C., Richards, L.J., and Suárez, R. (2020). Differential timing of a conserved transcriptional network underlies divergent cortical projection routes across mammalian brain evolution. *Proc. Natl. Acad. Sci. USA* *117*, 10554–10564.
29. Schneider, C.A., Rasband, W.S., and Eliceiri, K.W. (2012). NIH Image to ImageJ: 25 years of image analysis. *Nat. Methods* *9*, 671–675. <https://doi.org/10.1038/nmeth.2089>.
30. Allan, C., Burel, J.-M., Moore, J., Blackburn, C., Linkert, M., Loynton, S., Macdonald, D., Moore, W.J., Neves, C., Patterson, A., et al. (2012). OMERO: flexible, model-driven data management for experimental biology. *Nat. Methods* *9*, 245–253. <https://doi.org/10.1038/nmeth.1896>.
31. Chen, G., Gulbranson, D.R., Hou, Z., Bolin, J.M., Ruotti, V., Probasco, M.D., Smuga-Otto, K., Howden, S.E., Diol, N.R., Proppson, N.E., et al. (2011). Chemically defined conditions for human iPSC derivation and culture. *Nat. Methods* *8*, 424–429.
32. Weise, A., and Liehr, T. (2009). Pre- and postnatal diagnostics and research on peripheral Blood, chorion, amniocytes, and fibroblasts. In *Fluorescence in situ hybridization (FISH) — application guide*, T. Liehr, ed. (Springer Berlin Heidelberg), pp. 113–122.
33. Seabright, M. (1971). A rapid banding technique for human chromosomes. *Lancet* *2*, 971–972.
34. Salamanca, F., and Armendares, S. (1974). C bands in human metaphase chromosomes treated by barium hydroxide. *Ann. Genet.* *17*, 135–136.
35. Chambers, S.M., Fasano, C.A., Papapetrou, E.P., Tomishima, M., Sadelain, M., and Studer, L. (2009). Highly efficient neural conversion of human ES and iPSC cells by dual inhibition of SMAD signaling. *Nat. Biotechnol.* *27*, 275–280.

STAR★METHODS

KEY RESOURCES TABLE

REAGENT or RESOURCE	SOURCE	IDENTIFIER
Antibodies		
rabbit anti-SOX2	BioLegend	Cat#630802; RRID:AB_2195784
rabbit anti-OCT3/4	Abcam	Cat#ab19857; RRID:AB_445175
rabbit anti-NANOG	Thermo Fisher	Cat#PA1-097; RRID:AB_2539867
rat anti-SSEA3	Thermo Fisher	Cat#MA1-020X; RRID:AB_2536686
mouse anti-TRA-1-60	Cell Signaling	Cat#4746; RRID:AB_2119059
mouse anti-ACTN2	Sigma-Aldrich	Cat#A7811; RRID:AB_476766
rabbit anti-TNNT2	Abcam	Cat#ab45932; RRID:AB_956386
mouse anti-GATA4	Santa Cruz	Cat#sc-25310; RRID:AB_627667
rabbit anti-GATA4	Cell Signaling	Cat#36966; RRID:AB_2799108
goat anti-GATA6	R and D Systems	Cat#AF1700; RRID:AB_2108901
goat anti-SOX17	R and D Systems	Cat#AF1924; RRID:AB_355060
mouse anti-NESTIN	Thermo Fisher	Cat#MA1-110; RRID:AB_2536821
goat anti-SOX1	Thermo Fisher; ICC Kit	Cat#A24354
rabbit anti-PAX6	Thermo Fisher	Cat#42-6600; RRID:AB_2533534
mouse anti-BRN2	Santa Cruz	Cat#sc-393324; RRID:AB_2737347
mouse anti-FOXG1	Thermo Fisher	Cat#PA5-26794; RRID:AB_2544294
guinea pig anti-MAP2	Synaptic Systems	Cat#188 004; RRID:AB_2138181
rat anti-CTIP2	Abcam	Cat#ab18465; RRID:AB_2064130
mouse anti-SATB2	Santa Cruz	Cat#sc-81376; RRID:AB_1129287
mouse anti-GFAP	Thermo Fisher	Cat#A-21282; RRID:AB_2535827
donkey anti-goat Alexa Fluor 647	Thermo Fisher	Cat#A21447; RRID:AB_2535864
donkey anti-mouse Alexa Fluor 488	Thermo Fisher	Cat#A21202; RRID:AB_141607
donkey anti-rabbit Alexa Fluor 555	Thermo Fisher	Cat#A31572; RRID:AB_162543
donkey anti-rabbit Alexa Fluor 488	Thermo Fisher	Cat#A21206; RRID:AB_2535792
goat anti-mouse Alexa Fluor 488	Thermo Fisher	Cat#A21042; RRID:AB_2535711
goat anti-rat Alexa Fluor 555	Thermo Fisher	Cat#A21434; RRID:AB_2535855
goat anti-guinea pig Alexa Fluor 647	Thermo Fisher	Cat#A21450; RRID:AB_2735091
Bacterial and virus strains		
CytoTune – iPS 2.0 Sendai Reprogramming Kit; Lot#L2160042	Thermo Fisher	Cat#A16517
Biological samples		
Sumatran rhino skin biopsy	This paper	N/A
Chemicals, peptides, and recombinant proteins		
Geltrex	Thermo Fisher	Cat#A1569601
Matrigel	Corning	Cat#356231
knockout serum replacement (KSR)	Thermo Fisher	Cat#10828028
mTeSR1	STEMCELL Technologies	Cat#05850

(Continued on next page)

Continued

REAGENT or RESOURCE	SOURCE	IDENTIFIER
TrypLE select enzyme	Thermo Fisher	Cat#12563011
Y-27632	Selleck Chemicals	Cat#SEL-S1049-10MM
N-2 supplement	Thermo Fisher	Cat#17502048
B-27 supplement	Thermo Fisher	Cat#11875093
SB431542	Reagents Direct	Cat##21-A94
Dorsomorphin	Biovision	Cat#1686-5
Neurobasal Medium	Thermo Fisher	Cat#21103049
ReLeSR	STEMCELL Technologies	Cat#05872
bFGF	PeproTech	Cat#100-18B
TGFβ1	PeproTech	Cat#100-21C
Polybrene	Merck	Cat#TR-1003-G
Fibroblast Growth Medium (FGM)	Lonza	Cat#CC-3130

Critical commercial assays

PSC cardiomyocyte differentiation kit	Thermo Fisher	Cat#A2921201
StemMACS Trilineage EndoDiff medium	Miltenyi Biotec	Cat#30-115-659
STEMdiff™ Cerebral Organoid Kit	STEMCELL Technologies	Cat#08570

Experimental models: Cell lines

HMGU-001-A hiPSCs	Heiko Lickert, Helmholtz Zentrum München, Munich, Germany	N/A
Sumatran rhino fibroblasts	This paper	N/A
Sumatran rhino iPSCs	This paper	N/A
mitomycin C-treated mouse embryonic fibroblasts	tebu-bio	Cat#MEF-MITC

Oligonucleotides

RID_FWD: 5'-AACATCCGTAATCYCACCCA-3'	Ewart et al., 2018 ¹⁴	N/A
RID_REV: 5'-GGCAGATRAARAATATGGATGCT-3'	Ewart et al., 2018 ¹⁴	N/A

Software and algorithms

ImageJ	Schneider et al., 2012 ²⁹	https://imagej.nih.gov/ij/
Omero	Allan et al. 2012 ³⁰	https://www.openmicroscopy.org/index.html
Ikaros V5.1	Metasystems	

Other

ultra-low attachment surface plates	Corning	Cat#3471
-------------------------------------	---------	----------

RESOURCE AVAILABILITY**Lead contact**

Further information and requests for resources and reagents should be directed to and will be fulfilled by the lead contact, Sebastian Diecke (Sebastian.Diecke@mdc-berlin.de).

Materials availability

All cell lines generated in this study are potentially available on request to the [lead contact](#). The availability depends on CITES and Nagoya protocol restrictions.

Data and code availability

Data: All data reported in the paper are available from the [lead contact](#) upon request.

Code: This paper does not report original code.

Any additional information related to this study is available from the [lead contact](#) upon request.

EXPERIMENTAL MODEL AND SUBJECT DETAILS

Sumatran rhinoceros kertam

The male Sumatran rhinoceros (SR, also known as hairy rhinoceros or Asian two-horned rhinoceros, Bornean subspecies, *Dicerorhinus sumatrensis harrisoni*), Kertam (also called Tam) was captured from the wild in August 2008, when he was roughly 20 years old. Subsequently, he was housed in the Tabin Wildlife Reserve Sabah in Lahad Datu, Malaysia where he died in May 2019. All medical procedures were legalized by the Sabah Wildlife Department and performed by authorized veterinarians.

Human cell lines

Human iPS cells HMGUi-001-A (<https://hpscereg.eu>) were derived from fibroblasts of a healthy woman and were obtained from Heiko Lickert (Helmholtz Zentrum München, Munich, Germany). HMGUi-001-A hiPSCs were maintained in custom-made Essential 8 Medium [DMEM/F12 HEPES (Thermo Fisher, #11330032) supplemented with L-ascorbic acid 2-phosphate (Sigma, #A8960), insulin (CS Bio, #C9212-1G or Sigma, #91077C-1G), human transferrin (Sigma, #T3705-1G), sodium selenite (Sigma, #S5261-10G), bFGF (PeproTech, #100-18B), TGFβ1 (PeproTech, #100-21C) and sodium bicarbonate 7.5% solution (Fisher Scientific, #25080-094), according to³¹] on cell culture dishes coated with Geltrex (Thermo Fisher, #A1569601) at 37°C, 5% CO₂, 5% O₂ and passaged every 3–4 days using PBS 0.5 mM EDTA solution (PBS/EDTA, Thermo Fisher, #14190250 and #15575020) in ratios of 1:6 and 1:12. Cell line identity was authenticated by genotyping (STR analysis, GenePrint® 10 System, Promega Corporation) after banking.

METHOD DETAILS

Derivation of SR primary fibroblast

The skin biopsy from the SR Kertam was taken under general anaesthesia in the *regio axillaris* during a general health and reproductive assessment. The biopsy area was widely disinfected with Octenisept Spray (TM, SCHÜLKE & MAYR GmbH, #121411) and the deep skin biopsy was achieved by using a biopsy punch device (KAI Medical, 4 mm in diameter, #BP-40F), sterile surgical forceps and a sterile scalpel. The recovered tissue was immediately transferred into cell culture medium [DMEM, high glucose, GlutaMAX (Thermo Fisher, #10566016) supplemented with 10% fetal bovine serum (FBS, biowest, #S1400), 1X Penicillin-Streptomycin (biowest, #L0022), 1X Antibiotic-Antimycotic (biowest, #L0010)] and shipped at 4°C. The wound was sewed with simple surgical suture using 3/0 seam material with a sharp needle (Supramid®, 3/0 HS23 - 0,45m B. Braun Petzold, #C0712256). The suture site was covered against flies and better wound healing with veterinary aluminum wound spray (Pharmamedico GmbH, #03691157).

Upon arrival in the cell culture lab, the biopsy was diced into small pieces and cultured in DMEM/TCM 199 [1:1, DMEM, high glucose, GlutaMAX, HEPES (Gibco, #32430027) : Medium 199, HEPES (Gibco, #22340020)] supplemented with 10% FBS and 2 ng/mL basic fibroblast growth factor (bFGF, Peprotech, #AF-100-18B) in humidified air at 38°C, 5% CO₂ and 5% O₂. After expansion of cells in culture, they were subcultured every 4–6 days, frozen in DMEM/TCM 199 (1:1) with 20% FBS and 10% DMSO, and subsequently stored in liquid nitrogen.

Species analysis

To verify the identity of our SR primary fibroblasts, we applied a standardized species identification test published by Ewart et al., 2018.¹⁴ In brief, a cryovial containing primary fibroblasts was quickly thawed using a 37°C water bath. The cell suspension was transferred into a 1.5 mL Eppendorf tube and centrifuged at 300xg for 5 min at room temperature. The supernatant was aspirated and the cell pellet washed once in 1 mL PBS. After centrifugation at 300xg for 5 min at room temperature, the cell pellet was resuspended in 300 μL PBS and genomic DNA (gDNA) automatically extracted using the Maxwell RSC Blood DNA Kit (Promega, #AS1400) and a Maxwell RSC instrument according to the manufacturer's instructions (quick protocol from point 2 on). gDNA was eluted in 85 μL and its concentration measured by nanodrop. Subsequently, PCR was performed in 50 μL reaction volume comprising 100 ng template DNA, 1 μL Phire Hot Start II DNA Polymerase (Thermo Fisher, #F-122S), 1X Phire Reaction buffer, 200 μM dNTP mix (Thermo Fisher #18427-013), 0.5 μM of each "universal rhino primers" (RID_FWD: 5'-AACATCCGTAAATCYCACCCA-3' and RID_REV: 5'-GGCAGATRAARAATATGGATGCT-3') applying the following cycling protocol: 30 s initial denaturation at 98°C, 30 cycles of 5 s denaturation at 98°C, 5 s annealing at 55°C, 5 s extension at 72°C, and 1 min final extension at 72°C. 9.6 μL of the PCR reaction was subjected to gel electrophoresis [2% TAE agarose gel, Roti-Gel Stain (Roth, #3865.2), 100 bp DNA ladder (NEB, #N3231L)] to validate

exclusive amplification of the species specific 230 bp cytochrome-b region. The remaining PCR reaction was purified using the GeneJet PCR purification kit (Thermo Fisher, #K0702) according to the manufacturer's instructions. The nucleotide sequence was confirmed by Sanger sequencing and alignment to the published sequence.

Proliferation analysis

To calculate the cell doubling rate, SR primary fibroblasts were plated on four 3 × 24-well-plates coated with attachment factor (3.0×10^4 cells/24-Well) in skin media. After 24, 48, 72, and 96 h, one 3 × 24-well-plate was fixed each. To this end, medium was aspirated, cells were washed once with PBS, and subsequently incubated for 15 min at room temperature in BD Cytofix solution (BD Biosciences, #554655). Afterwards, cells were washed three times and stored in PBS. Plates were sealed with parafilm and kept in the fridge in the dark until further use.

When all time points were collected, cells were incubated slowly shaking for 30 min at room temperature in staining solution [PBS with 0.1% Triton X-100 (Carl Roth, #3051.3), 2 drops/mL DAPI (NucBlue Fixed cell Stain Ready Probe, Thermo Fisher, #R37606)]. Subsequently, cells were washed three times with PBS. Per timepoint, 3 images (1 image per 24-well) were acquired with a LEICA DIMI8 microscope and the LAS X Software (10x magnification, 500 milliseconds exposure time). Single nuclei were automatically counted using ImageJ software.

Generation of SR-iPSCs

After thawing, SR primary fibroblasts were maintained at 37°C and 5% CO₂ on cell culture plates coated with attachment factor (Thermo Fisher, #S006100) in skin media [DMEM, high glucose, GlutaMAX, pyruvate supplemented with 10% FBS, 1X MEM non-essential amino acids (NEAA, Thermo Fisher, #11140035) and 10 ng/mL bFGF]. With minor changes, reprogramming was performed as described previously for the northern white rhino (Hayashi et al. *submitted*;¹⁵). In brief, two days before transduction (day -2), fibroblasts were detached by incubation with TrypLE select enzyme (Thermo Fisher, #12563011) for 8 min at 37°C, and 2.4×10^4 cells were plated each in 3 × 12-wells coated with attachment factor in skin media. On the next day, medium was changed. On the day of transduction (day 0), cells of 1 × 12-well were detached with TrypLE and counted ($\sim 9.25 \times 10^4$ cells).

Based on the obtained cell number, the amount of Sendai viruses (CytoTune – iPS 2.0 Sendai Reprogramming Kit, Thermo Fisher, #A16517, Lot #L2160042) needed for transduction of cells in 1 × 12-well with an multiplicity of infection (MOI) of 10:10:6 (KOS:c-Myc:Klf4) was calculated. The medium of 2 × 12-wells was changed to skin medium containing 10 µg/mL polybrene (Merck, #TR-1003-G). Sendai virus mixture was added to 1 × 12-well. The other 1 × 12-well was not transduced and served as negative control. The plate was sealed with parafilm and centrifuged at room temperature and 800xg. After 20 min centrifugation, the plate was turned and centrifuged for another 10 min. Subsequently, parafilm was removed and the plate incubated overnight at 37°C and 5% CO₂. On the next day (day 1), cells were washed once with skin medium and subsequently fed with skin medium. Skin medium was changed on day 2, day 4 and day 6. On day 7, transduced cells were carefully detached by incubation with TrypLE for 2–3 min at 37°C, and 5 different numbers of transduced cells (1.5, 3.0, 5.0, 7.5, 10.0 × 10³) were plated on 5x6-wells [coated with Geltrex and laid with 2.0 × 10⁵ mitomycin C-treated mouse embryonic fibroblasts (MEFs, tebu-bio, #MEF-MITC)] in skin medium. Additionally, 20 × 10³ and 40 × 10³ cells were plated feeder-free on Geltrex coated 2x6-wells. On the next day (day 8) medium of cells plated on MEFs was changed to KB medium [39% DMEM, high glucose (Thermo Fisher, #41965039), 39% complete FGM (Lonza, #CC3132), 20% knockout serum replacement (KSR, Thermo Fisher, #10828028), 1x NEAA, 1x GlutaMAX (Thermo Fisher, #35050061), 0.1 mM 2-Mercaptoethanol (Thermo Fisher, #21985023), and 12 ng/mL bFGF], whereas feeder-free cultures were changed to mTeSR1 medium (STEMCELL Technologies, #05850). From now on, medium was changed daily. On day 19, 8 and 4 single colonies were picked from KB on MEFs and feeder-free mTeSR1 wells, respectively. One promising clone observed in KB media on MEFs was split into 2 halves. One half was picked on day 19 (line #8), the other one on day 21 (line #9). Additionally, 2 and 5 individual colonies were isolated on this day from KB on MEFs and feeder-free mTeSR1 conditions, respectively. Depending on the previous culturing condition (KB or mTeSR1), picked single colonies were transferred to individual Geltrex coated 24-wells, which were either laid with 5.0 × 10⁴ MEFs/well or kept feeder-free, respectively. The culturing media (KB or mTeSR1) was supplemented with 10 µM ROCK inhibitor (Y-27632, Selleck Chemicals, #SEL-S1049-10MM) at the day of picking and on the day after. Three lines

(#8, #9, #14; #8 and #9 were isolated from the same original clone) – all originating from KB on MEFs conditions - grew successfully and displayed nice morphology. The other lines could not be propagated further and were discarded. For splitting, cultures were incubated for 7–8 min at 37°C in PBS/EDTA. KB medium was supplemented with 10 μM ROCK inhibitor for 24 h after splitting. Line #8, #9, #14 were cryopreserved in KSR, 10% Dimethyl Sulfoxid (DMSO, Sigma, #D22660). Subsequent experiments were performed with line #9.

Clearance of sendai-virus encoded RNA

To generate vector-free SR-iPSC lines, we picked 12 subclones from line #9 at passage 4 on individual Geltrex coated 24-wells laid with 5.0×10^4 MEFs/well. KB medium was supplemented with 10 μM ROCK inhibitor for 24 h after picking. All subclones were expanded and samples for RNA extraction collected at passages 7, 8 and 9. RNA was isolated using the RNeasy Mini Kit (Qiagen, #74106) according to the manufacturer's instructions. RNA was eluted in 40 μL water and its concentration measured by Nanodrop. 3 μL of each sample were reversely transcribed with SuperScript III First-Strand Synthesis SuperMix (Thermo Fisher, #18080400) using oligo(dT) primer and following the corresponding protocol of the manufacturer. cDNA was diluted 1:5 with water and 2 μL used for PCR [20 μL reaction volume, DreamTaq Green PCR Master Mix (Thermo Scientific, #K1081), 0.5 μM each forward and reverse primer, primer sequences provided in the manual of the CytoTune – iPSC 2.0 Sendai Reprogramming Kit (Thermo Fisher, #A16517); PCR program: 5 min initial denaturation at 94°C, 35 cycles of 30 s denaturation at 95°C, 30 s annealing at 55°C, 30 s elongation at 72°C, followed by final extension for 7 min at 72°C]. Absence of Sendai-virus encoded genes (SeV, KOS, Klf4, c-Myc) was confirmed by gel electrophoresis (2% TAE agarose gel, Roti-Gel Stain, 100 bp DNA ladder) for subclones #9A, #9C and #9K at passages 7 (#9A and #9C) and 9 (#9K). Subsequent experiments were performed with line #9K.

SR-iPSC maintenance culture

SR-iPSCs were cultured on Geltrex or attachment factor coated cell culture dishes laid with MEFs (21–29 cells/cm²) at 37°C and 5% CO₂. When cells reached 80–90% confluency, they were split with PBS/EDTA (6–7 min at 37°C) in varying ratios (1:3–1:12). ROCK inhibitor was added to the medium at 5 μM for the first 24 h after passaging.

Karyotyping of SR-iPSCs

To check the genomic integrity of SR-fibroblasts and SR-iPSCs, Giemsa-trypsin-Giemsa (GTG, G-banding) banding technique was performed as described in Hayashi et al. *submitted* (according to^{32,33}). Additionally, centromeric heterochromatin staining (CBG, C-banding) was performed following a protocol adapted from.³⁴ The methods are briefly summarized below.

Chromosome preparation

SR-fibroblasts were split with TrypLE (incubation for 8 min at 37°C) and 2.5×10^5 cells were plated each in two T25flasks coated with attachment factor. Cells were fed with skin media, which was changed every other day. SR-iPSCs were detached with PBS/EDTA for 6–7 min at 37°C and 6.25×10^5 cells were plated each in two Geltrex coated T25flasks in cKB supplemented with 5 μM ROCK inhibitor, which was changed daily.

At 50% confluency, cells were treated with 0.1 g/mL colcemide (Biochrom AG, #L6221) for 2.5 h at 37°C, and subsequently harvested using Trypsin-EDTA (Biochrom AG, # L2143). Enzymatic digestion was stopped by adding medium containing 10% KSR. Cells from two T25 flasks were pooled in one 50 mL Falcon tube and centrifuged at room temperature for 5–10 min at 450xg. The supernatant was discarded except for 1 mL, which was used to resuspend the cell pellet and to transfer it into a 15 mL falcon tube. Cells were treated with 10 mL hypotonic 0.075 M KCl solution (Merck, #1049360500) for 20 min at 37°C, followed by adding ~1 mL freshly prepared ice-cold fixative (Methanol/Acetic acid, ratio 3:1, Merck, #1060092500 and #1000632500) and careful mixing. After centrifugation at room temperature for 5–10 min at 450xg, the supernatant was discarded except for ~1 mL to resuspend the cell pellet. Subsequently, cells were washed three times with 5–10 mL fixative, centrifuged and finally resuspended in 2 mL fixative and stored at –20°C. Before slides were prepared, the cell pellet was washed again and resuspended in fresh fixative. The cell suspension was dropped on a cleaned, cooled and wet glass slide, air dried and baked over night at 70°C for subsequent GTG and CBG banding.

GTG banding

Slides were processed in a glass cuvette at room temperature with 1 mL trypsin stock solution (Gibco, #27250–018, 6 g in 100 mL in PBS Dulbecco, Biochrom, #L1825) diluted in 100 mL PBS for 2 s, put in a glass cuvette with 150 mL buffer pH 6,88 (Merck, # 1072941000) and transferred to a second glass cuvette with 150 mL buffer pH 6,88. Subsequently, slides were stained in a glass cuvette with Giemsa solution [6 mL Giemsa stain (Sigma, # GS500) and 75 mL buffer pH 6,88] for 3 min, rinsed with aqua deion. and finally air dried. Metaphase chromosomes were automatically scanned and imaged with the Zeiss Axio.Z2 microscope using the scanning system Metafer and the Ikaros V5.1 software (both Metasystems). The average resolution was ~200 bands per haploid chromosome set. In total, 10–20 metaphase spreads were analyzed per cell line.

CBG banding

For CBG, slides were treated with 0.2 N hydrochloric acid (Merck, # 109057) for 1 h at room temperature, rinsed with aqua deion., incubated for 7 min in filtered 5% barium hydroxide solution (Merck, #101737), rinsed again with aqua deion., left for 5 min in 0.2 N hydrochloric acid followed by 1 h incubation in 2xSSC (Invitrogen, # 15557–036) at 60°C, rinsed with aqua deion., stained with Giemsa stain solution for 20 min, finally rinsed with aqua deion. and air dried. Ten metaphases were captured under an Axioskop 20 light microscope (Zeiss) at 100x oil immersion objective and analyzed by Ikaros V5.1 software (Metasystems).

Three germ layer differentiation potential

Endoderm was differentiated from SR-iPSCs using the StemMACS Trilineage EndoDiff medium (Miltenyi Biotec, #30-115-659) following the manufacturer's instructions. In brief, SR-iPSCs were detached with PBS/EDTA and resuspended in 1 mL MEF conditioned KB medium (cKB) supplemented with 10 μ M ROCK inhibitor. cKB was generated by incubating MEFs overnight in KB medium (2 mL per 2×10^5 MEFs/6-well). 2-Mercaptoethanol and FGF were added freshly before using the medium on SR-iPSCs. The cell suspension was filtered through a 70 μ m strainer (Miltenyi Biotec, #130-095-823) and single living cells counted using Trypan Blue (Thermo Fisher, #T10282) and the CellDrop Bright Field Cell Counter (Biozym, # 31CELLDROPBF-UNLTD). Subsequently, 1.25×10^5 cells were plated per Geltrex coated 24-well (containing cover slip) in 0.5 mL cKB medium supplemented with 10 μ M ROCK inhibitor (day 0). On day 1, 0.5 mL cKB medium without additional ROCK inhibitor was added. On day 2, medium was changed to EndoDiff medium. On day 3–6, EndoDiff medium was changed daily. On day 7, cells were washed twice in PBS+/+ (PBS, calcium, magnesium; Thermo Fisher, #14040141), and subsequently fixed for 15 min at room temperature in BD cytofix solution (BD, #554655). After washing twice in PBS+/+, fixed cells were stored at 4°C until further use.

To represent the mesoderm, SR-iPSCs were differentiated into cardiomyocytes using a PSC cardiomyocyte differentiation kit (Thermo Fisher, #A2921201) according to the manufacturer's instructions. In brief, SR-iPSCs were detached with PBS/EDTA and plated in cKB supplemented with 1X RevitaCell (Thermo Fisher, #A2644501) in various ratios (corresponding to 1:4–1:12) in Geltrex coated 12-wells. For the next two days, cells were fed daily with cKB without RevitaCell. Day 3 after plating, medium was changed to Cardiomyocyte Differentiation Medium A (day 0). On day 2, the medium was slowly aspirated and carefully 2 mL pre-warmed Cardiomyocyte Differentiation Medium B was added per well. On day 4, cultures were cautiously shaken to swirl up dead cells, medium was removed, and 2 mL pre-warmed Cardiomyocyte Maintenance Medium added per well. From now on, Cardiomyocyte Maintenance Medium was changed every other day. Clusters of beating cells were observed from day 9 on. Around day 11, cultures were changed to RPMI B-27 medium [RPMI 1640 (Thermo Fisher, #11875093) supplemented with B-27 (Thermo Fisher, #17504044)], which was changed every other day. After day 15, cardiomyocytes were fixed as described before and stored at 4°C until further use.

The neural (ectodermal) differentiation of SR-iPSCs was induced by a modified version of the dual SMAD inhibition protocol published by Chambers et al., 2009.³⁵ In brief, SR-iPSC were detached with PBS/EDTA and 6.0×10^5 cells plated per 6-well in cKB supplemented with 5 μ M ROCK inhibitor. On the next day, medium was changed to cKB without ROCK inhibitor. The day after (day 0), medium was changed to neural induction medium [NIM; DMEM/F12 (Thermo Fisher, #12660012), 1x B-27, 1x N-2 (Thermo Fisher, #17502048), 10 μ M SB431542 (Reagents Direct, #21-A94), 2 μ M Dorsomorphin (Biovision, #1686–5)]. NIM was exchanged daily for 5 consecutive days. On day 6, cells were washed once with PBS and subsequently detached using Accutase (Thermo Fisher, #A1110501). Enzymatic reaction was stopped after 8 min by adding neural expansion medium [NEM; 0.5X advanced DMEM/F12 (Thermo Fisher, #12634010), 0.5X

Neurobasal Medium (Thermo Fisher, #21103049); 2X N-2 (Thermo Fisher, #17502048)] supplemented with 5 μ M ROCK inhibitor. Cells were detached using a cell scraper and passed through a 70 μ m strainer and subsequently centrifuged at 300xg for 3 min at room temperature. The supernatant was discarded, cells resuspended in NEM supplemented with 5 μ M ROCK inhibitor, counted, and 1×10^5 cells plated per Geltrex coated 24-well (containing cover slip). Medium was changed every day with NEM. On day 12, cells were fixed as described previously and stored at 4°C until further use.

Cerebral organoids

Cerebral organoids with mainly cortical identity were generated from SR-iPSCs with the STEMdiff™ Cerebral Organoid Kit (STEMCELL Technologies, #08570) based on a previously described protocol¹⁸ with some modifications during EB formation (days 0–5). Briefly, SR-iPSC grown in clusters on MEFs were detached using ReleSR (STEMCELL Technologies, #05872) according to the manufacturer's instructions. Detached cell aggregates of 50–200 μ m size were transferred to a 15 mL tube using a 5 mL serological pipette. After settling down, medium was removed, aggregates resuspended in 2 mL KB medium, plated in one well of a 6-well plate with ultra-low attachment surface (Corning, #3471) and kept at 37°C and 5% CO₂. KB medium was changed on days 1 and 3 by transferring the EBs to a 15mL tube as described above. From day 5 on, the timing and the media of the organoid kit were used, with exception of day 7, where 2% Matrigel (Corning, # 356231) was added to the medium for neuroepithelial expansion, instead of droplet embedding of single EBs. On day 10, the medium was exchanged for maturation medium and organoids were placed on an orbital shaker rotating at 65 rpm in the incubator from there on.

Cryosectioning of cerebral organoids

Organoids between 1 and 3 months of age were fixed in 4% PFA (Affimatrix, #199431LT) for 30 min at room temperature, washed 3 times in PBS and left overnight at 4°C in 30% sucrose solution. Next day, organoids were embedded in warmed 7.5% gelatin solution (VWR, # 24350.262), cooled down on ice, snap frozen in isopentane/dry ice (–50°C) and stored at –80°C, according to Lancaster et al. 2014.¹⁸ Organoids were cryosectioned in 20 μ m thick slices using a MicroM HM 560 Cryostat (Thermo Fisher), collected on Superfrost Ultraplus glass slides (Roth, #H867.1) and stored at –80°C.

Immunofluorescence

To stain SR-iPSCs in pluripotent state or after 2D-differentiation into cells of the three germ layers, cells were fixed as described previously. PBS+/+ was aspired and cells blocked for 1 h shaking at room temperature either in 1xPBS+/+, 5% normal goat serum (NGS; Abcam, #ab7481) for surface markers, or for intracellular and nuclear markers in blocking buffer [PBS+/+, 0.2% BSA (Biomol, # 1400100), 0.3% Triton X (Sigma, #T8787), 10 x NGS or rather normal donkey serum (NDS, abcam, #ab7475)].

For immunohistochemical analysis of cryosectioned organoids, gelatin was removed from the slides by incubation in PBS at 42°C (three times à 20 min). Subsequently slides were rinsed in PBS, 0.3% Triton-X100 and blocked in blocking buffer for 1 h shaking at room temperature.

After blocking of cells or rather organoid slides, primary antibodies were diluted as indicated in [Table S1](#) in 1xPBS+/+, 1% BSA for surface markers or blocking buffer for intracellular and nuclear markers. After incubation overnight shaking at 4°C, samples were washed three times à 15 min in PBS+/+. Secondary antibodies were diluted in PBS+/+ containing DAPI, and samples incubated in the solution for ~2 h shaking at room temperature. Subsequently, samples were washed three times in PBS+/+. Cells grown on cover slips and organoid slides were mounted using Fluoromount-G (Thermo Fisher, #00-4958-02). Images were captured and processed with a Leica DMI8 microscope and the LASX software (including THUNDER computational clearing method).

QUANTIFICATION AND STATISTICAL ANALYSIS

Data shown in [Figure 1A](#) comprises of three replicates per time point. Per timepoint, data for each replicate (circle) and mean (line) are depicted. For karyotyping, 10–20 metaphase spreads were analyzed per cell line.